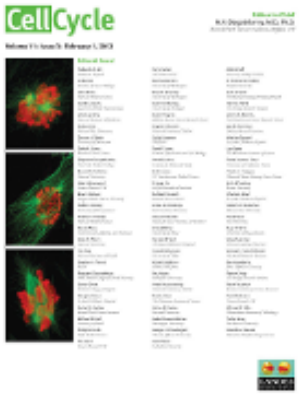

Cell Cycle
Publication details, including instructions for authors and subscription information:
http://www.tandfonline.com/loi/kccy20

The metallophosphodiesterase Mpped2 impairs tumorigenesis in neuroblastoma

Lucia Liguori, Immacolata Andolfo, Paqualino De Antonellis, Veruska Aglio, Valeria di Dato, Natascia Marino, Nicola Ivan Orlotti, Daniela De Martino, Mario Capasso, Giuseppe Petrosino, Alexander Schramm, Luigi Navas, Gian Paolo Tonini, Angelika Eggert, Achille Iolascon & Massimo Zollo

Published online: 14 Feb 2012.

To cite this article: Lucia Liguori, Immacolata Andolfo, Paqualino De Antonellis, Veruska Aglio, Valeria di Dato, Natascia Marino, Nicola Ivan Orlotti, Daniela De Martino, Mario Capasso, Giuseppe Petrosino, Alexander Schramm, Luigi Navas, Gian Paolo Tonini, Angelika Eggert, Achille Iolascon & Massimo Zollo (2012) The metallophosphodiesterase Mpped2 impairs tumorigenesis in neuroblastoma, Cell Cycle, 11:3, 569-581, DOI: 10.4161/cc.11.3.19063

To link to this article: http://dx.doi.org/10.4161/cc.11.3.19063

Cell Cycle 11:3, 569-581; February 1, 2012; © 2012 Landes Bioscience

The metallophosphodiesterase Mpped2 impairs tumorigenesis in neuroblastoma

Lucia Liguori,[1,2] Immacolata Andolfo,[1,2] Pasqualino de Antonellis,[1,2] Veruska Aglio,[1,2] Valeria di Dato,[1,2] Natascia Marino,[1,2] Nicola Ivan Orlotti,[1,2] Daniela De Martino,[1,2] Mario Capasso,[1,2] Giuseppe Petrosino,[1] Alexander Schramm,[3] Luigi Navas,[4] Gian Paolo Tonini,[5] Angelika Eggert,[3] Achille Iolascon[1,2] and Massimo Zollo[1,2,*]

[1]CEINGE; Biotecnologie Avanzate; [2]Department of Biochemistry and Medical Biotechnology; [4]Pathology and Animal Health; Section of Pathological Anatomy; Faculty of Veterinary Medicine; 'Federico II' University of Naples; Naples, Italy; [3]Department of Paediatric Haematology/Oncology; University Children's Hospital; Essen, Germany; [5]Translational Paediatric Oncology and Italian Neuroblastoma Foundation; National Cancer Research Institute; Genova, Italy

Key words: Mpped2, neuroblastoma, retinoic acid, gene expression, xenograft

Abbreviations: 13-cis-RA, 13-cis-retinoic acid; ATRA, all-trans retinoic acid; MB, medulloblastoma; NB, neuroblastoma; PDE, cyclic nucleotide metallophosphodiesterase

Through microarray analyses, we identified the *Mpped2* gene as differentially expressed in two neuroblastoma cell lines induced to differentiation with all-trans retinoic acid. *Mpped2* codes for a new metallophosphodiesterase protein, the expression of which inhibits cell proliferation and soft agar colony formation in SH-SY5Y cells. This inhibition is concomitant to an increased proportion of the cells in G_0/G_1 phase and enhanced caspase 3 activation, effects not seen for the other phosphodiesterases. A Mpped2-null mutation (H67R) abrogates these functions, which indicates that the biochemical activity of Mpped2 is advantageous for cancer suppression. Expression analyses in the "Los Angeles" and "Essen" neuroblastoma gene-array data sets show that increased expression of *Mpped2* is associated with good patient prognosis according to Kaplan-Meier analyses. Tumorigenic assays in mice show that overexpression of *Mpped2* improves survival rate, substantially impairs tumor growth and induces neuronal differentiation. Altogether, these data show that *Mpped2* expression impairs neuroblastoma tumorigenesis, and they establish a basis for future therapeutic applications.

Introduction

Neuroblastoma (NB) represents the most frequent extra-cranial solid neoplasia in children, and it is responsible for about 15% of all pediatric cancer deaths. It is an embryonic malignancy of the postganglionic sympathetic nervous system that generally arises in one of two locations: the adrenal medulla or the paraspinal sympathetic ganglia.[1] The clinical hallmark of NB is its large heterogeneity; indeed, NB shows diverse clinical and biological characteristics and behavior.[2-4] The treatments used in the management of NB include surgery, chemotherapy and radiotherapy. Most pediatric clinical trials stratify patients into different groups at diagnosis based on the many risk factors, such as age at diagnosis, International NB Staging System stage, tumor histopathology and *MYCN* gene status.[1,5]

Retinoic acid is an essential factor derived from vitamin A, and during embryonic development in normal tissues, it has been shown to have a variety of functions in cell differentiation, proliferation and apoptosis.[6] All-trans retinoic acid (ATRA) has been used as a chemotherapeutic agent with some success,[7] although 13-cis-retinoic acid (13-cis-RA) is preferred due to its more favorable pharmacokinetics.[8-10] Indeed, a phase I trial showed that higher and more sustained drug levels are obtained with 13-cis-RA relative to ATRA.[7] High levels of either ATRA or 13-cis-RA can cause arrest of cell growth and morphological differentiation of human NB cell lines.[7] A phase III, randomized trial showed that high-dose, pulse therapy with 13-cis-RA after completion of intensive chemoradiotherapy (with or without autologous bone-marrow transplantation) significantly improves event-free survival for patients with high-risk NB.

The retinoic acids affect NB differentiation through transcriptional regulation of genes that are either directly involved in the differentiation process or that control the differentiation process.[11-13] Gene expression profiling on NB specimens has identified molecular signatures for high-risk and low-risk tumors[14-16] and novel prognostic markers.[17-19] We investigated the expression profile of NB cell lines induced to differentiation using ATRA to identify early target genes that are involved in this transcriptional network.

Through this screening, we identified the *Mpped2* gene (also known as c11orf8 or 239FB), which shows high expression in differentiated NB cells. The *Mpped2* gene is located on human chromosome 11p13 between the *FSHB* and *PAX6* genes in a region that is also associated with Wilms' tumor, aniridia, genitourinary anomalies and mental retardation (WAGR syndrome).[20,21] *Mpped2* mRNA is predominantly expressed in fetal brain,[22]

*Correspondence to: Massimo Zollo; Email: massimo.zollo@unina.it
Submitted: 12/09/11; Accepted: 12/14/11
http://dx.doi.org/10.4161/cc.11.3.19063

and the high degree of similarity between the predicted protein sequences of Mpped2 and those of two *Caenorhabditis elegans* cDNA clones demonstrates that there is extensive evolutionary conservation of Mpped2 as a family of class III metallophosphodiesterase in mammals.[23]

The cyclic nucleotide phosphodiesterases (PDEs) are an important enzyme class that hydrolyzed the cyclic nucleotides to 5'-AMP and 5'-GMP. These enzymes are significantly different in primary amino acid sequence and can be categorized into three classes (I–III).[24,25] The class I enzymes are, so far, the most characterized in higher eukaryotes and have been extensively studied at the biochemical and structural level.[26] The class II enzymes have been identified in a few organisms, such as yeast, Dictyostelium and Vibrio.[24] The third class was first identified in *Escherichia coli* as the regulator of the lactose operon, also called the Icc or CpdA protein.[27] This latest class of enzymes has remained largely unexplored, while a related enzyme from Hemophilus has been identified that lacks a biochemical characterization.[28,29] *Mpped2* gene representes the first evidence for a class III cyclic nucleotide phosphodiesterase in mammals.[30]

PDEs, classes I and II, have been studied in a variety of tumors, and the data suggest that PDE activity is elevated in tumors, thus affecting the ratio of cAMP to cGMP in tumor cells. In addition, PDE inhibitors are potential targets for tumor cell growth inhibition, induction of apoptosis, impairment of early inflammatory insults,[31] modulation of T-cell responses[32] and monocytic differentiation[33] and increases in chemotherapeutic efficacy.[34] Abnormalities due to overexpression of PDEs cause dysregulation of cAMP and/or cGMP signaling and pathway activation, leading to promotion of tumor formation. Additionally, this impairment of cAMP and/or cGMP generation by overexpression of PDE isoforms has been described in various cancer pathologies, e.g., overexpression of PDE11A and PDE8B (showing genetic predisposition to adrenocortical hyperplasia tumors[35,36]) and of h-Prune, which is implicated in breast cancer metastasis and colon, pancreas, gastric and esophageal cancers.[36,37]

In the present study, we demonstrate that Mpped2 reduces cell proliferation and anchorage-independent growth and induces apoptosis. Results are also confirmed in vivo using xenograft NB models. These data support an anti-tumorigenic function for Mpped2, and unlike some of the other PDEs isolated to date, this shows that Mpped2 has a role in the impairment of cancer progression. In agreement with our in vitro and in vivo studies, we also show here that expression of *Mpped2* in NB tumors decreases during disease progression in patients, thus identifying a potential new molecular target for future therapeutic applications.

Results

Gene expression studies. Following gene expression analyses of two independent NB cell lines, LAN-5 and SH-SY5Y cells, we focused our attention on the *Mpped2* gene, which showed early upregulation during a short pulse of ATRA-induced differentiation in both of these cell systems. The *Mpped2* gene is highly transcribed in fetal brain, maps to the chromosome 11pter > 11p15.1 region and is known to be deleted in less than 4% of NBs analyzed (14/394).[38] The rat fetal brain gene "*rat 239FB*" is a homolog of human *Mpped2*, and it has been shown to retain a hydrolytic activity against cAMP, thus representing the first mammalian protein appertaining to the class III cyclic nucleotide metallophosphodiesterases. Despite the large number of metallophosphodiesterases isolated from eukaryotes, their functions and those of their specific substrates in mammals remain to be identified, with no natural substrates recognized for many of them.[39,40] The histidine 67-to-arginine (H67R) mutation of Mpped2 abrogates its cAMP-linearization PDE activity in vitro.[30] This mutation is located in the large C-terminal domain of Mpped2 (from H57 to S294), which contains the conserved residues of the metallophosphodiesterase superfamily and a typical phosphoprotein-phosphatase-like fold. The crystal structure of Mpped2 was recently described in a detailed analysis of full-length rat Mpped2.[41]

Relative gene expression of *Mpped* in human tissue and tumor cell lines. We analyzed *Mpped2* expression in 16 different cell lines, which included four human medulloblastoma cell lines (D283, D341, DAOY, UW228),[42,43] two breast cancer cell lines (MDA231T, MDA435), one cervical cancer cell line (HELA) and 11 NB cell lines [IMR-32, SK-N-BE (2), LAN-5, GILIN, KELLY, LAN-1, NB69, NGB, SHEP, SH-SY5Y, SK-N-AS],[44-46] (**Fig. 1A**). For the NB cell lines, there was specific expression of *Mpped2* mainly during differentiation in the LAN-5, GILIN and NB69 cells, with low expression in the SH-SY5Y and IMR-32 cells. In the medulloblastoma cell lines, only the D283 cells showed detectable levels of *Mpped2* expression.

The levels of *Mpped2* showed higher expression in 14 different adult human tissues compared with five fetal tissues and especially for those derived from the central nervous system (CNS) (e.g., cerebellum, frontal cortex, total brain) (**Fig. 1B**), providing support to some previous studies.[22] Some other tissues, such as the thyroid gland, are known to express significant levels of *Mpped2*.[47]

To confirm this specific expression in the CNS, we determined the levels of expression of the murine *Mpped2* homolog gene (*NM_198778.2*) in six mouse tissues at different stages of development (E.14.5, E.16.5, P.0) (**Fig. 1C**). Indeed, this *Mpped2* homolog gene showed elevated expression in the CNS, limbic system and eyes. In particular, its expression levels increased during embryonic development, with higher expression at stage 16.5E in brain tissue, while in heart and kidney, the peak of expression was at E14.5. Overall, these data suggest a role for *Mpped2* mRNA expression during the cell proliferation and differentiation processes that occur in these tissues of nervous system origin.

Overexpression of Mpped2 correlates with a neuronal differentiation phenotype in NB cells. To determine whether endogenous *Mpped2* is differentialy regulated during neural differentiation induced by 48 h ATRA treatment, we used immunofluorescence and western blotting to analyze endogenous Mpped2 in SH-SY5Y NB cells. This was also repeated for ATRA treatment of the LAN-5 and SK-N-BE (2) NB cell lines. Differentiation of the NB cells was shown using a neuronal differentiation marker as control (the neurofilament light polypeptide). The immunofluorescence data using the S1 anti-Mpped2 antibody showed

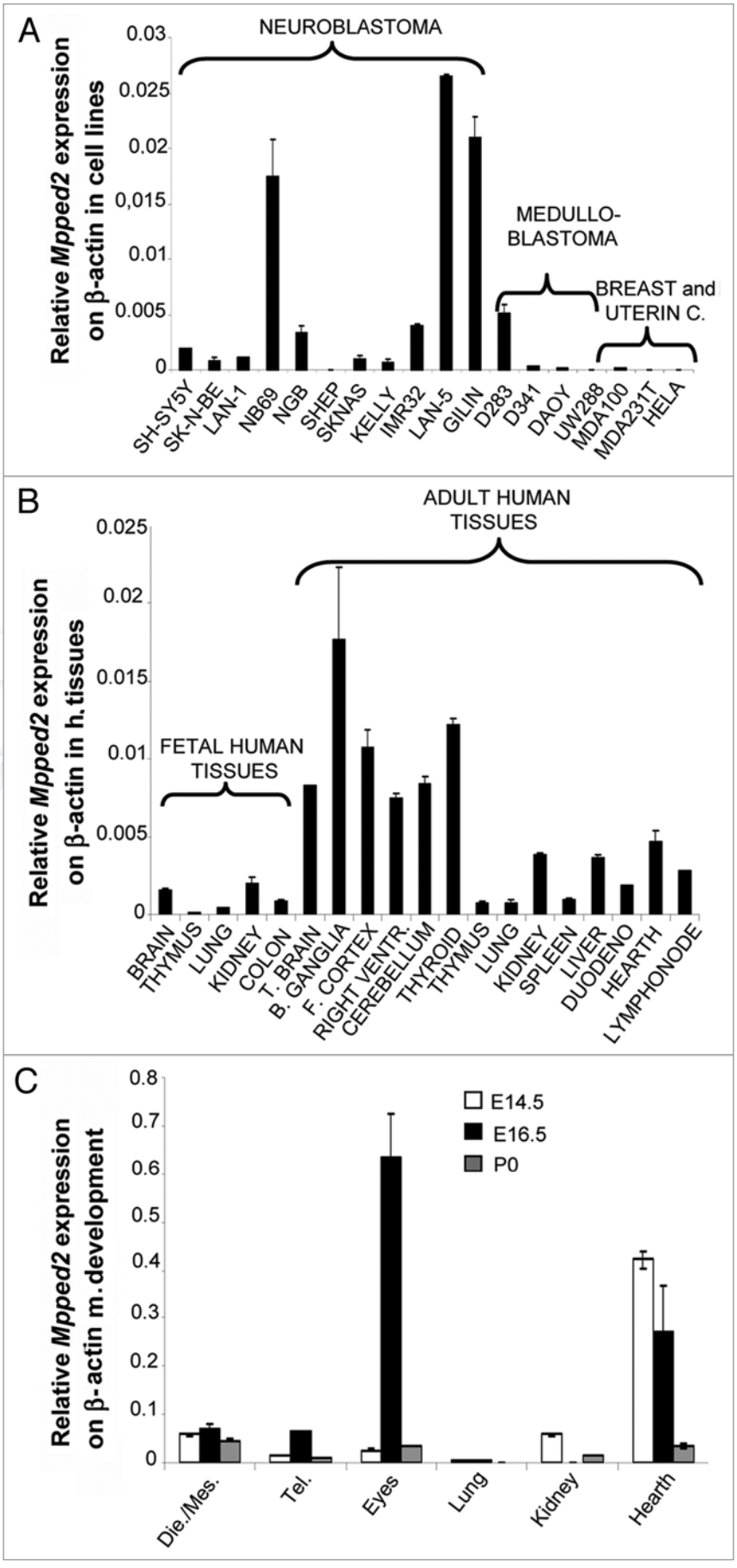

Figure 1A–C. Relative *Mpped2* gene expression in human tissues, tumor cell lines and murine tissues and localization in differentiated NB cell lines. (A) Relative *Mpped2* gene expression by RT-PCR in NB, medulloblastoma, breast cancer and cervical uterine cell lines (as indicated). (B) Relative *Mpped2* gene expression by RT-PCR in 14 adult human tissues and in five fetal human tissues (as indicated). (C) Relative *Mpped2* gene expression by RT-PCR in six mouse tissues (as indicated) at three different stages of development (E14.5, E16.5, P0). TEL, telencephalon; DIE, diencephalons; MES, mesencephalon. Relative expression levels for each RT-PCR were calculated against expression of the β-actin gene.

Mpped2 expression in the cytosolic compartment of SH-SY5Y NB cells, with a more pronounced localization in the perinuclear region when Mpped2 was expressed under the ATRA-induced differentiation (**Fig. 1D**). Moreover, these immunofluorescence studies revealed upregulation of Mpped2 expression during this in vitro ATRA-induced neural differentiation in SK-N-BE (2) NB cells (**Fig. 1D**). Similar results were obtained in these SH-SY5Y and SK-N-BE (2) cells by western blotting (**Fig. 1E**), thus indicating that expression of the Mpped2 protein is upregulated after 48 h of neural differentiation induced by ATRA. **Figure S1A** shows the levels of upregulation of differentiation marker expression (Nestin, Tuj1, synaptophysin, RAR-α, RAR-β) for the in NB *Mpped2* #4 and *Mpped2* #7 stable clones (see next paragraph). These results provide further support for this Mpped2-induced differentiation in NB cells.

Overexpression of Mpped2 induces G_0/G_1 arrest in SH-SY5Y cells. We also generated several stable clones for the production of Mpped2 in SH-SY5Y cells. **Figure S1B** shows the level of *Mpped2* in three stable clones (*Mpped2* #4, #7 and #9) also assayed by western blotting using the S1 anti-Mpped2 antibody (**Fig. S1C**). Because *Mpped2* #4 showed higher expression of Mpped2, we used this clone for propidium iodide staining and fluorescent cell sorting (FACs analyses). The *Mpped2* #4 clone showed a significant increase in the G_0/G_1 cell population and a decrease in the S-phase cell population as compared with a stable clone that overexpresses the H67R-mutated *Mpped* (**Fig. 2B**). In fact, we also generated several stable clones that overexpress the H67R-mutated *Mpped2* (**Fig. S1D**) and, using RT-PCR, we selected the clone that showed higher expression of *Mpped2*. This *Mpped2* H67R mutation has previously been reported to negatively affect Mpped2 metallophosphodiesterase catalytic

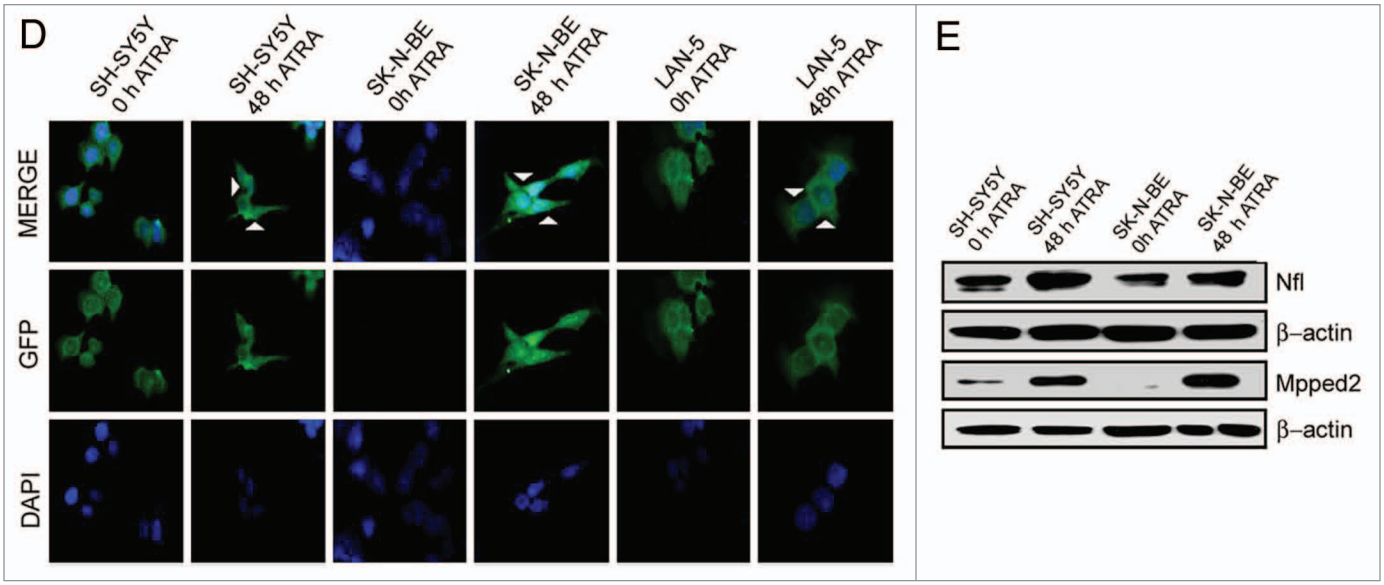

Figure 1D and E. (D) Immunofluorescence analyses showing upregulation of Mpped2 expression during in vitro neural differentiation of NB cell lines (as indicated) stimulated by ATRA. White arrowheads, cytosolic compartment and perinuclear positive staining. (E) Representative western blot showing upregulation of Mpped2 expression during in vitro neural differentiation in SK-N-BE (2) and SH-SY5Y NB cell lines stimulated by ATRA. Nfl, neurofilament light polypeptide, a neuronal differentiation marker.

activity.[30,41] As a control, we assayed the Mpped2 H67R mutant for its cAMP-PDE activity.[48] As recently described in reference 41, the structure of the Mpped2 H67R mutant differs from that of the wild-type protein in terms of the position of its W182. While in the wild-type protein, this W182 residue points into the solvent, it is turned toward the center of the active site in the Mpped2 H67R mutant due to the absence of bound nucleotide, which thus explains its lack of PDE activity. As shown in **Figure 2A**, the *Mpped2* #4 stable clone has significant cAMP PDE activity over the *Mpped2*-H67R #8 stable clone (*p = 0.007). These *Mpped2*-H67R mutant clones also did not show any variation in their relative G_0/G_1 populations when compared with the *Mpped2* #4 cell population (**Fig. 2B and C**), thus indicating that these changes in the cell cycle seen with overexpression of Mpped2 indeed arise through the Mpped2 catalytic activity.

Furthermore, we used sh-interference (*sh*) ribonucleotide methodology for *Mpped2* silencing (see **Sup. Materials**). Using four different ribonucleotides (#9, #10, #11, #12) (**Fig. S1F**) upon *sh-Mpped2* transfection, the SH-SY5Y cell line showed dramatically reduced levels of *Mpped2.* FACS analyses of the sh#11-*Mpped2*-transfected SH-SY5Y cells indicated a reduction in the G_0/G_1 population by 20% of the control cells (**Fig. 2D**). In addition, these sh#11-*Mpped2*-transfected cells showed an increase of 11% in the S-phase component of the cell cycle, with little change in the G_2/M phase. Similar results were obtained from the analysis of the sh#9-*Mpped2*-transfected cells (**Fig. 2D**).

Therefore, RT-PCR and western blotting were used to examine the effects of Mpped2 on some genes involved in the control of the cell cycle. For this reason, we used RT-PCR to determine if this was the case in our Mpped2-overexpressing clones. We examined the basal levels of mRNA of selected cell cycle-related proteins (cyclin D1, p21 and $p27^{kip}$). Expression data for members of the cyclin mRNA in three different *Mpped2* stable clones relative to the SH-SY5Y control cells are shown in **Figure S2E**. There were clearly lower levels of cyclin D1 mRNA expression with increased levels of p21 mRNA (**Fig. S2E**). No differences were seen from the controls for the expression levels of the CDK inhibitor p27. We also observed a reduced expression of cyclin D1 in the *Mpped2* #4 stable clone as compared with the wild-type SH-SY5Y cells and the SH-SY5Y cells overexpressing the mutation *Mpped2* H67R (**Fig. 2E**).

We can conclude here that in these NB cells overexpressing Mpped2, there is an arrest at the G_0/G_1 phase of the cell cycle. These effects on the cell cycle are most likely due to the Mpped2 cAMP metallophosphodiesterases activity, as the Mpped2 H67R mutation abrogated the G_0/G_1 cell cycle arrest.

Mpped2 overexpression impairs proliferation and anchorage-independent growth of SH-SY5Y cells by inducing apoptosis. Proliferation assays were performed with the SH-SY5Y cells, the *Mpped2* #4 clone and the *Mpped2*-H67R #8 clone using the MTS [3-(4,5-dimethylyhiazol-2-yl)-5-(3-carboxymethoxyphenyl)-2-(4-sulfophenyl)-2H-tetrazolium] colorimetric assay methodology (see **Sup. Materials**). Here, there was a significant decrease in proliferation of the *Mpped2* #4 clone with respect to the *Mpped2*-H67R #8 clone that overexpresses the Mpped2 H67R mutant (**p = 0.0002; **Fig. 2F**). These data again confirm that the PDE activity of Mpped2 is involved in this function.

With the arrest in G_0/G_1 phase of the cell cycle shown for these Mpped2-overexpressing clones, we asked whether Mpped2 also acts on the apoptosis signaling cascade. Thus, we assayed caspase activity in the absence and presence of staurosporine isolated from the bacterium *Streptomyces*, a natural product that is known to activate caspase-3. In the *Mpped2* #4 clone there was a significant increase in caspase activity with respect to both the

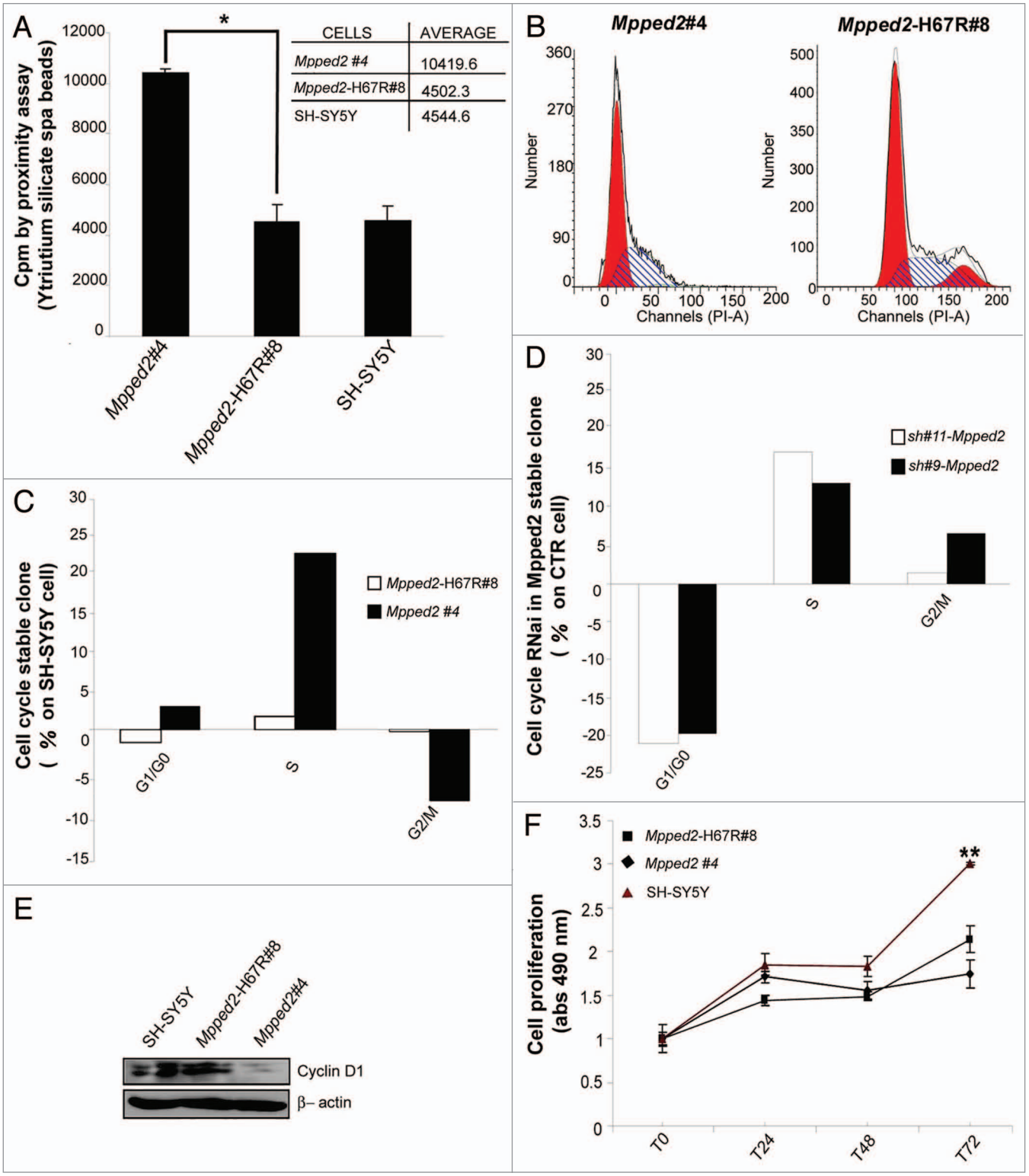

Figure 2. *Mpped2* overexpression induces G_0/G_1 arrest in SH-SY5Y cells. (A) The *Mpped2* #4 stable clone shows a greater cAMP-PDE activity compared with the empty vector clone and the *Mpped2*-H67R #8 stable clone, as measured by PDE scintillation proximity assay. Inset: mean proximity assay cpm for the different clones. (B) The *Mpped2* #4 clone (left) shows a significantly greater G_1/S ratio for the cell population compared with the *Mpped2*-H67R #8 clone (right), as determined by propidium iodide staining and fluorescent cell sorting. (C and D) Relative percentages of the different *Mpped2* clones (as indicated) in the different phases of the cell cycle, showing the *Mpped2* #4 and *Mpped2*-H67R #8 clones (C) and the sh#11-*Mpped* and sh#9-*Mpped* (D) clones. (E) Representative western blot shows low expression of cyclin D1 in the *Mpped2* #4 clone, as compared with the wild-type SH-SY5Y cells and the *Mpped2*-H67R #8 clone. (F) Proliferation of the *Mpped2* #4 stable clone, as compared with the wild-type SH-SY5Y cells and the *Mpped2*-H67R #8 clone, according to absorbances from the MTS colorimetric assay (see Materials and Methods). Data are means ± SD of two independent experiments, each performed in triplicate **p = 0.0002.

SH-SY5Y cell line (*p = 0.040) and the *Mpped2*-H67R #8 clone (*p = 0.015) (**Fig. 3A**).

Furthermore, to determine if Mpped2 affects the ability of these cells to grow without the need for attachment to a surface, thus potentially enhancing the anchorage-dependent activity of these cells, we performed soft agar assays with the SH-SY5Y cells and the *Mpped2* #4 clone and the *Mpped2*-H67R #8 clone over 3 weeks (see **Sup. Materials**). Here, there was a substantial significant reduction in the number of colonies for the *Mpped2* #4 clone compared with both the SH-SY5Y cells (***p = 0.0000008) and the *Mpped2*-H67R #8 clone (***p = 0.0004) (**Fig. 3B**). These results confirm that Mpped2 can restore anchorage-dependent growth of the SH-SY5Y cell line, with this function again related to its cAMP-metallophosphodiesterase activity.

In vivo tumorigenic assay in athymic nude mice. The Mpped2 H67R mutation abrogates Mpped2 PDE activity in vitro.[30,34,41] To determine whether this mutation can also abrogate the in vivo function of the wild-type Mpped2 protein observed previously in vitro, we performed a flank tumorigenesis assay in athymic nude mice. Four mice (M1, M2, M3, M4) were inoculated subcutaneously in their paired right and left flanks with the human NB SH-SY5Y cells, as the *Mpped2* #4 clone and the *Mpped2*-H67R #8 clone. After nine weeks, significant differences in the sizes and weights were seen between the tumors generated in the flanks injected with the *Mpped2* #4 clone with respect to those generated with the *Mpped2*-H67R #8 clone (**Fig. 3C**). The tumors explanted from these mice were smaller in size from the *Mpped2* #4 clone as compared with tumors generated by the *Mpped2*-H67R #8 clone (**Fig. 3D**), with a significant difference in the mean weights between these tumors (***p = 0.00015) (**Fig. 3E**). **Table 1** gives the individual *Mpped2* #4 and *Mpped2*-H67R #8 tumor weights along with the means and standard deviations.

In summary, the H67R mutation of the Mpped2 protein reversed the anti-proliferative phenotype of the wild-type Mpped2 protein in NB, which thus enhanced the in vivo tumorigenesis. Therefore, the wild-type Mpped2 metallophosphodiesterase PDE activity has an anticancer function that needs to be further investigated for future therapeutic applications.

Xenograft NB analysis of Mpped2-overexpressing cells. We then investigated a xenograft animal model of NB to determine whether Mpped2 is an inhibitor of tumor progression in vivo. For this, we mimicked the NB tumorigenesis in athymic/nude animals following methodologies described previously in reference 49. We cloned HA-tagged wild-type *Mpped2* cDNA and a control HA-tagged pcDNA empty vector in the SH-SY5Y cell line, together with an expression vector that carried luciferase cDNA, which produced several stable clones (see Material and Methods). These clones were tested for luciferase expression levels (as shown in **Fig. S2A and B**). The stable *Mpped2* #9-p*Luc*#1, with higher expression of *Mpped2* and luciferase, and Ctr-p*Luc*#2 SH-SY5Y clones were then injected into the supra-adrenal glands of 16 athymic/nude mice ("*Mpped2-Luc* #1-#8 mice" and "Ctr-*Luc* #1-#8 mice"; the Crt-*Luc* #8 and *Mpped2-Luc* #4 mice died on day 0, after injection of the cells). Weekly, in vivo measurements of the bioluminescence imaging (BLI) signals of these clone-injected mice were used to evaluate the tumor growth. At eight weeks, all the mice showed a visible tumor mass; however, smaller tumor masses were seen for the *Mpped2-Luc* mice as compared with the Ctr-*Luc* mice. Overall, significantly higher levels were seen for the BLI signals and the sizes of these tumors for the Ctr-*Luc* mice compared with the mice injected with the *Mpped2*-overexpressing *Mpped2-Luc* cells (**Fig. 4A and B**). Note also in **Figure 4A** that the injections of the Ctr-*Luc* cells resulted in tumors that were not only macroscopically bigger than those seen for the *Mpped2-Luc* mice, but also further distributed throughout the body as signs of metastasis. These BLI signals were observed weekly and were used in the statistical analyses based on animal groups that showed similar baseline signal intensities of luciferase (at time zero of injection; see **Table S1**). These are shown in **Figure 4B** as a box plot for the comparisons of the BLI signals between the Ctr-*Luc* (#1, #2, #4 and #7) mice and the *Mpped2-Luc* (#1, #5, #7 and #8) mice that were injected with the *Mpped2*-overexpressing cells (**Fig. 4B**). Thus, the mice carrying the *Mpped2* overexpressing cells showed less tumor burden over this time of tumorigenesis in vivo.

In these Ctr-*Luc*- and *Mpped2-Luc*-induced xenograft tumors, immunohistochemistry analyses were also performed to characterize the expression levels of some markers known to be involved in cell proliferation and differentiation: Tuj1, Nestin and Ki67. As shown in **Figure 4C**, for these explanted tumors after 59 d in vivo, compared with the Ctr-*Luc* #2 tumor, positive staining for Tuj1 and Nestin was decreased in the *Mpped2-Luc* #7 tumor, indicative of enhanced cell differentiation. This was accompanied by a relative decrease in the Ki67 staining in the *Mpped2-Luc* #7 tumor, indicative of decreased cell proliferation.

Taken together, these data show that the Mpped2 protein impairs tumor formation in vivo in these athymic/nude mice, which corresponds to decreased cell proliferation (according to Ki67 staining) and enhanced cell differentiation (according to Tuj1 and Nestin staining). Therefore, the lower tumor growth in mice that received the supra-adrenal injections of Mpped2-overexpressing cells can be ascribed to the pro-differentiation function of Mpped2, as was shown for these marker proteins in vitro (**Fig. S1A**). These analyses allow us to define an additional level of tumor impairment for the Mpped2 protein in vivo, as shown in this animal xenograft model of NB.

Expression of Mpped2 in tumors and its association to prognosis of NB. We then investigated whether *Mpped2* gene expression has a major role in NB tumor progression. Here, we analyzed the expression of the *Mpped2* gene in different data sets that are available in the public online database Oncomine (available at https://www.oncomine.org/resource/login.html). In the "Wang" and "Shai Brain" data sets, we noted that *Mpped2* expression is negatively correlated with malignant brain tumors both in NB and glioblastoma.[50,51]

We then analyzed 33 NB tissues for *Mpped2* mRNA expression using RT-PCR (see **Sup. Materials, Methods**). We divided these *Mpped2* genetic data for the NB samples into two groups according to the NB stage: 15 mild (1, 2, 4s) and 17 aggressive (3 and 4) tumors. Analyses of these extrapolated *Mpped2* expression values showed that they were higher for NB stages 1 and 2, as compared with the later stages of development of this cancer,

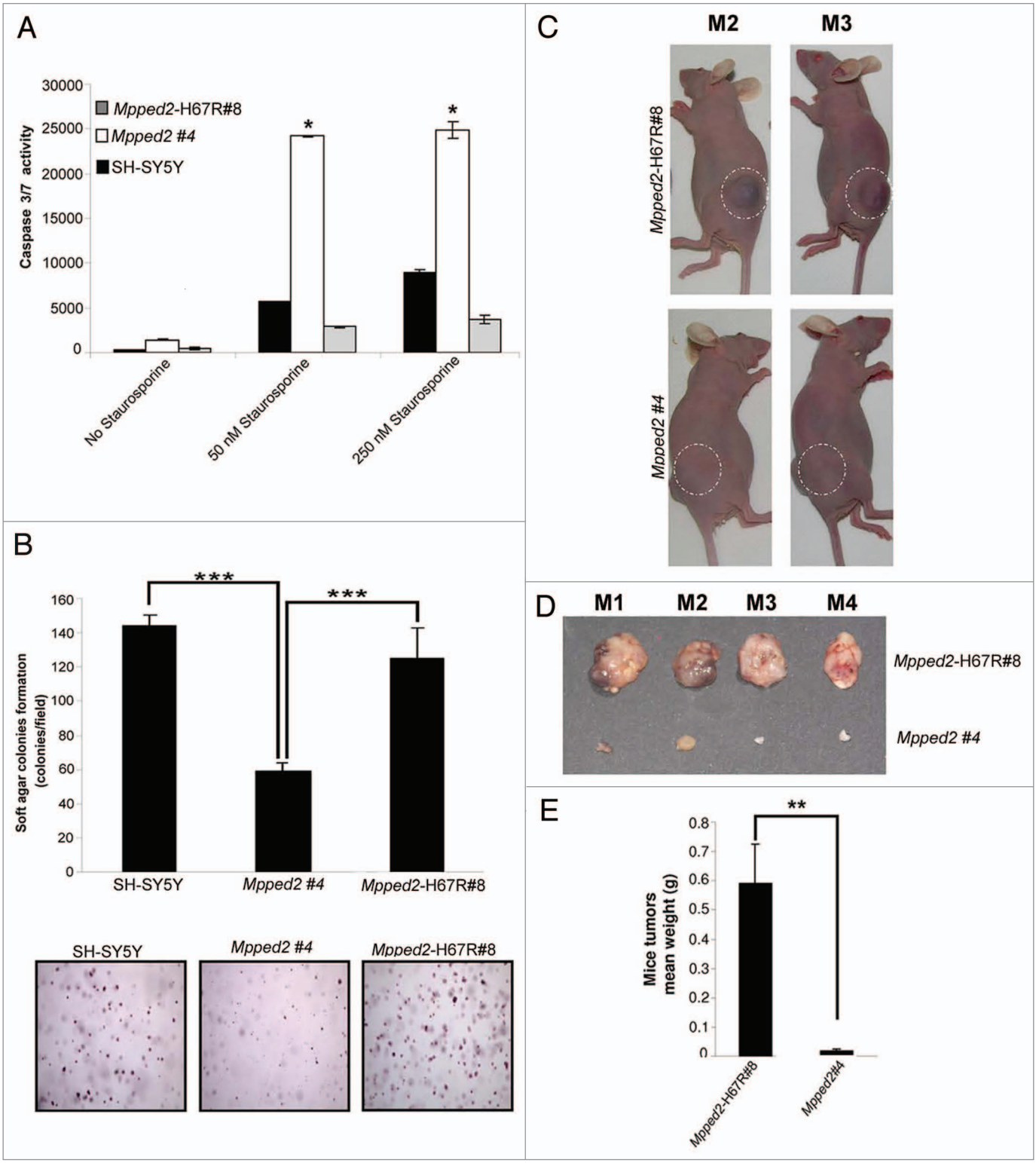

Figure 3. Proliferation, apoptosis and anchorage-independent growth assays and the flank xenograft NB model. (A) Caspase 3/7 activity assays (see Sup. Materials, Methods) in the absence and presence of staurosporine for the *Mpped2* #4 clone, as compared with the wild type SH-SY5Y cells and the *Mpped2*-H67R #8 clone (as indicated). (B) Soft agar assay. Top: The number of colonies for the *Mpped2* #4 stable clone, as compared with wild type SH-SY5Y cells and the *Mpped2*-H67R #8 cells. Data are means ± SD of two independent experiments, each carried in triplicate. *p ≤ 0.05. Bottom: Representative photographs of these colonies (as indicated). (C) Two representative athymic nude mice (#2 and #3), with right and left flank injections of the *Mpped2* #4 and *Mpped2*-H67R #8 stable clones, respectively. (D) Explanted tumors from the flanks of the four mice (#1–#4) that had the right and left flank injections of the *Mpped2* #4 and *Mpped2*-H67R #8 stable clones. (E) Mean weights of the tumors in (D), according to the *Mpped2* #4 and *Mpped2*-H67R#8 clones injected. Data are means ± SD of each set of four tumors (as indicated). **p = 0.00015.

Table 1. Tumor weights from the *Mpped2* #4 and *Mpped2*-H67R #8 injections of the paired double-flank tumorigenesis xenografts after nine weeks in vivo, in the four independent nude mice

Mouse	Tumor weight (g)	
	***Mpped2* #4 (right flank)**	***Mpped2*-H67R #8 (left flank)**
#1	0.012	0.722
#2	0.031	0.52
#3	0.014	0.682
#4	0.012	0.433
Mean	**0.01725**	**0.58925**
Standard deviation	**0.009215**	**0.135935**

although this difference did not reach statistical significant (p = 0.24; data not shown). We believe that this lack of significance is due to the relative low number of samples that we could analyze here. However, in the Kaplan-Meier survival analysis, the loss of expression of *Mpped2* in the advanced tumor stages (3 and 4), indeed, significantly correlated with worse prognosis (**Fig. 4D**; *p = 0.023). Similarly, box-plot analysis in the same cohort of patients showed that higher expression of *Mpped2* significantly correlated with patient death (**Fig. S3A**; *p = 0.02).

We then ask if these phenomena can be seen for other previously published gene expression signatures of NB.[52] Comparing here the "Los Angeles" (GEO accession number GSE3446) and the "Essen" data sets (see Materials and Methods), *Mpped2* levels in 110 patients without disease relapse (mean, 8.45 ± 1.06; median, 8.67) were significantly higher when compared with 74 patients with disease relapse (mean, 7.99 ± 1.34; median, 8.20; **Fig. S3B**; Mann Whitney test; *p = 0.027). All of these NB patients had metastatic tumors that lacked *MYCN* gene amplification. Overall, these data show correlations between *Mpped2* expression and advanced NB tumor progression, and they support our in vitro studies in mice that show that *Mpped2* expression is mainly lost in advanced stages of NB, thus correlating these findings with an impairment of tumorigenesis that is driven by the biochemical metallophosphodiesterase function of Mpped2 in NB.

Epigenetic regulation of Mpped2 expression as a possible mechanism for silencing. As there is downregulation of *Mpped2* expression in advanced NB tumors, we then asked about the regulation of *Mpped2* expression in NB tumorigenesis on the basis of epigenetic regulation.

To identify evidence of epigenetic regulation in NB, we compared *Mpped2* gene expression in the two NB cell lines SHSY-5Y, SK-N-BE (2) and in a breast cancer cell line (MB-MDA231T) in the absence and presence of the demethylation agent 5'-aza-2'-deoxycytidine (AZA). Here, the levels of mRNA expression of the *Mpped2* gene increased significantly after 48 h and 72 h of AZA treatment of these NB cell lines (SH-SY5Y, *p = 0.046; SK-N-BE (2), *p = 0.028; **Fig. S3C**, see **Sup. Materials**) and of these MB-MDA231T breast cancer cells (*p = 0.046; **Fig. S3D**; see **Sup. Materials, Methods**). These data indicate that epigenetic regulation, such as methylation of CpG islands upstream of the *Mpped2* promoter region, most likely represents the mechanism of silencing by Mpped2 during cancerogenesis.

Discussion

We have sought here to fully characterize *Mpped2* expression in human tissues of neuronal origin, with confirmation from publically available, in silico data (see also the GEO profiles in the UNIGENE source database). Initially, our analysis of murine tissues at different embryonic stages showed that *Mpped2* expression is modulated during development. Here, we noted that *Mpped2* is highly expressed in brain, and particularly between the 16.5 and P0 d of development. These data strengthened our choice to focus on this particular gene to further extend its characterization and to ascribe a potential functional role for Mpped2 in neuronal differentiation processes that occur at 14.5 d during the development of the CNS.

We also show that Mpped2-overexpressing clones of SH-SY5Y cells show reduced cell proliferation. Cell cycle analysis shows that in these stable Mpped2-overexpressing clones, there is an increase in the population of cells in the G_1/G_0 phase, which leads to a significant increase in the G_1/S ratio. These data were confirmed by cell cycle analysis in SH-SY5Y and LAN-5 cells overexpressing the myc-EGFP-Mpped2 construct (see **Sup. Materials**). An opposite situation was observed in the *Mpped2*-H67R clones, thus underlining that the Mpped2 metallophosphodiesterase cAMP activity is directly involved in its anti-proliferative function. The cell cycle is a highly regulated process that involves a complex cascade of cellular events, including mainly activation of cyclins and cyclin-dependent kinases (CDKs).[53] For example, the CDK/cyclin D complex promotes progression through G_1 into S phase.[53,54] In addition, the activities of the CDK/cyclin complexes are negatively regulated by binding to CDK inhibitors, such as the Cip/Kip family of proteins (p21, p27, p57).

At present, it is known that a number of neuronal determinants affect cells at the G_1 phase, allowing them to then follow differentiation via the G_0 branch. In addition, it is known that external neuronal determination signals, such as Wnt, Sonic Hedgehog and retinoic acid receptor (RAR) signaling, can regulate cell cycle exit through the modulation of cyclin D1, cyclin D2 and *MYCN* transcription.[55-58] In agreement with previous data, *Mpped2* appears to promote cell cycle exit by silencing cyclin D1 and $p27^{kip}$ while enhancing p21 expression. Further investigations are needed to determine whether this lower expression of cyclin D1 is directly linked to *Mpped2* overexpression and, thus, whether this will influence cell cycle control through a not-yet-characterized mechanism of action. The immunofluorescence studies and western blotting here reveal upregulation of *Mpped2* expression during ATRA-induced in vitro neural differentiation in SK-N-BE(2) and SH-SY5Y NB cells. With this cell cycle arrest of the *Mpped2* #4 stable clone, we asked whether Mpped2 can activate the apoptosis cascade. These data indicate that in the Mpped2-overexpressing *Mpped2* #4 clone, there is an increase in caspase activity as

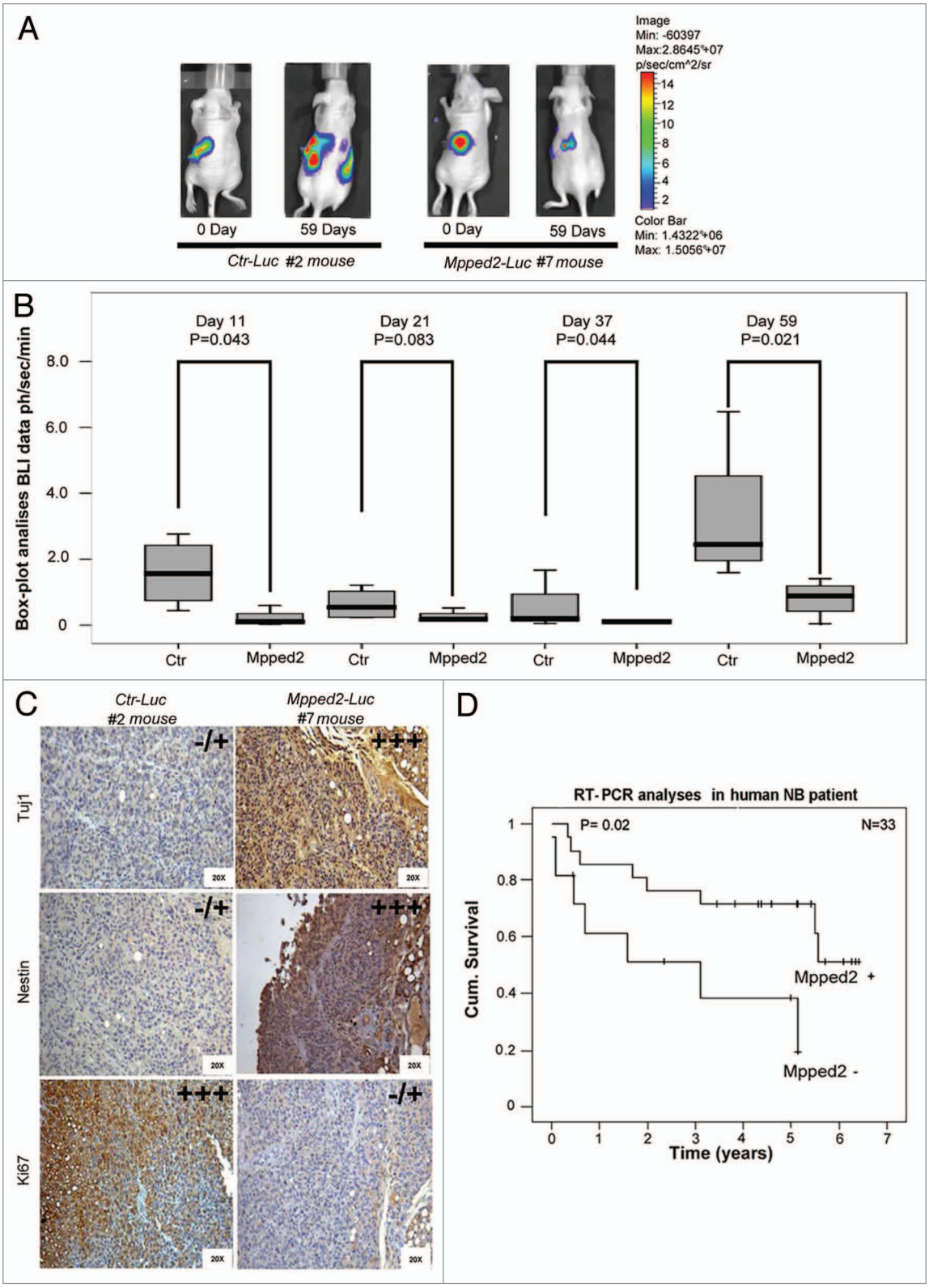

Figure 4. For figure legend, see page 578.

Figure 4 (See opposite page). Xenograft neuroblastoma model. Differentiation and proliferation markers and correlation of *Mpped2* expression with tumor aggressiveness in NB patients. (A) Represenative xenograft NB model of tumorigenesis eight weeks afer s.c. injection with the Ctr-*Luc* #1 cells in mouse #2 (Ctr) and the *Mpped2* #9-*Luc* #2 cells in mouse #7, as measured by BLI signals according to the color bar shown. (B) Time course of the mean tumor sizes of the tumors from the injections of the Ctr-*Luc* and *Mpped2-Luc* cells in terms of mean BLI signals for the pooled data (photons/s, as fold-increases over day 0), as shown in **Table S1**. Statistical evaluation was by two-tailed, unpaired t-tests. (C) Representative immunohistochemistry analyses after day 59 of the xenograft tumors from the Ctr-*Luc* mouse #2 and *Mpped2-Luc* mouse #7, for the differentiation markers Tuj1 and Nestin, and the proliferation marker Ki67. (D) Kaplan-Meier curves for patient survival probability related to the 33 human NB tumors. Mpped2^{+} (n = 15) and Mpped2^{-} (n = 18) indicate patients with tumors that contained high and low levels of Mpped2, respectively, as determined by RT-PCR. *p = 0.02; significance for expression of Mpped2 as a predictor for improved survival at a 7-y follow-up.

compared with the SH-SY5Y cell line and the *Mpped2*-H67R #8 clone.

Altogether, these data support the functional significance of *Mpped2* upregulation as it relates to cell cycle inhibition, induction of apoptosis and differentiation of neuronal precursors, representing unique opposite functions with respect to other known phosphodiesterases appertaining to class I and II. We thus speculate that this "opposite" behavior of Mpped2 as a PDE in NB is associated with its PDE function. Thus, maintenance of low levels of *Mpped2* expression during tumor progression would appear to be essential for a proliferative cellular precursor state, whereas high *Mpped2* expression would be required for arrest of cell proliferation, with differentiation then taking place. How *Mpped2* expression is regulated during the switch from proliferation to differentiation will be the topic of future studies.

Thus, our findings indicate that the lost of the *Mpped2* gene is a new molecular marker for the definition of a new unfavorable risk class. This is supported by our "in vivo" xenograft studies, which confirm the anti-proliferation function of Mpped2 in vivo. Indeed, mice carrying an overexpressing *Mpped2* gene in NB cells were seen to have a low aggressive phenotype in the tumor xenograft model of neuroblastoma.

According to the literature, *Mpped2* is downregulated in the expression profiling of malignant vs. benign papillary thyroid carcinoma,[59] and in particular, *Mpped2* is part of a group of 11 genes that are informative and discriminating for benign and malignant lesions in thyroid tumors.[60] Additionally, in breast cancer, *Mpped2* has been shown to be downregulated in >50% of breast tumors and in ~20% of lymph node metastases, which additionally show lower levels of *Mpped2* expression when compared with normal breast tissue.[61]

Two mechanisms of regulation of *Mpped2* anti-tumorigenesis function have been raised at this time. Our present study suggests epigenetic regulation of Mpped2 expression, as this increases after treatment with AZA in NB and breast cancer cell lines. A second mechanism is implied by the hypothesis that the acquired mutation (H67R) of Mpped2 can impair its catalytic metallophosphodiesterase activity, which can then influence its antiproliferative function. This mutation is a single nucleotide polymorphism (SNP) in the SNP database (rs11556749) with genotype frequencies of A/A 0.983 and A/G 0.017 in the European population. Our analysis for the genotype A/G in 33 NB samples using direct PCR sequencing of the gene in these tumors (data not shown) will not have detected the heterozygous genotype in these patients because of the rare frequency of this genotype (A/G) in the European population. Indeed, if the mutation occurs, and if it is sufficient as heterozygote status, we would expect a higher probability to develop NB tumors, and future studies should address this hypothesis.

Indeed, in our studies in mice carrying wild-type *Mpped2* cells, these showed a significant reduction in tumor growth in comparison with those carrying the *Mpped2*-H67R #8 stable clones. These data further support the role of the *Mpped2*-H67R mutation in vivo and strength our first hypothesis.

A question can be raised at this time. Can we increase the levels of *Mpped2* expression in tumorigenic cells for future therapeutic development? The consequence of these increased levels of *Mpped2* expression is an impairment of the normal cell cycle growth conditions, thus finally enhancing the potential anticancer activity of Mpped2. These data augment our findings and definitively emphasize the need to search for the catalytically specific metallophosphodiesterase function of Mpped2. Here, the results obtained recently for a three-dimensional structure are very encouraging,[30] and studies on molecular Mpped2 structure data will be able to identify new small molecules that enhance its catalytic function.

These studies thus shed light on this new marker, Mpped2, and there is now the need to address its potential benefit for therapeutic use to impair cancer progression.

Materials and Methods

Cell culture, vector cloning, real-time quantitative PCR, western blotting, immunofluorescence analyses, proliferation assays, epigenetic assays, flank injections, immunohistochemistry, cell cycle analysis and patient follow-up data are all available in the **Supplemental Materials**.

In silico analyses of Mpped2 gene expression on two independent NB data sets. The first set of expression data for the *Mpped2* gene is available on the public online database Gene Expression Omnibus (GEO) (www.ncbi.nlm.nih.gov/sites/entrez; accession number GSE3446). This data set, which comes from the Children's Hospital Los Angeles (Affymetrix Human Genome U133A and U133B Array, United Kingdom), contains the gene expression profiling of 102 metastatic NB that do not show amplification of the *MYCN* oncogene; we have referred to this as the "Los Angeles" data set. We divided the sample in two groups: 56 patients without disease relapse and 46 with occurrence of disease relapse. The second data set was provided by the University Children's Hospital, Essen, Germany. In brief, total RNA was isolated from 101 primary NB samples that were obtained prior to therapy, and it was hybridized to the Human Exon 1.0 ST array (Affymetrix), according to the manufacturer protocol. From the 101 primary neuroblastomas, we selected the

gene expression profiles of 38 metastatic NB that lack amplification of *MYCN*, and we divided them into two groups of 17 patients without disease relapse and 21 patients with disease relapse. We have referred to these data as the "Essen" data set. The values for both data sets are given as log2 of normalized expression. The significant difference of the *Mpped2* expression between the two groups was assessed by the Mann Whitney test.

PDE assay. PDE activity was measured using a cAMP/cGMP detection assay (Sigma Aldrich), as described by D'Angelo et al. and with a scintillation proximity assay (Amersham Pharmacia Biotech). The cAMP standard curves were constructed using commercial Phosphodiesterases I from *Crotalus atrox* (Sigma Aldrich). The samples were diluted as required and incubated at 30°C in 100 μl assay buffer (50 mM TRIS-HCl [pH 7.4], 8.3 mM $MgCl_2$, 1.7 mM EGTA) containing the desired concentrations of cAMP or cGMP as substrate (3:1 ratio as unlabeled to [^{3}H]-labeled). All of the reactions, including the buffer-only blanks, were conducted in duplicate and allowed to proceed for an incubation time that resulted in 25% substrate turnover (empirically determined). The reactions were terminated by adding 50 μl Yttrium silicate scintillation proximity assay beads (Amersham Pharmacia Biotech). The enzyme bioactivities were calculated for the amount of radiolabel product detected according to the manufacturer protocol.

NB tumorigenic assays in athymic nude mice. *Flank xenograft mice implantation.* Four athymic nude mice (M1, M2, M3, M4) were inoculated subcutaneously in their right and left posterior flanks with the human NB cells SH-SY5Y, as the Mpped2 #4 stable clone and as the Mpped2-H67R #8 clone, respectively (see **Sup. Material, Methods**). These NB cells were injected to a volume of 100 μl of PBS, containing a total of 2 x 10^6 cells. The mice were followed for tumor growth for 9 weeks, and then they were sacrificed, and the tumor tissues were dissected out and analyzed.

Supra-adrenal xenograft mice implantation. The stable SH-SY5Y cells overexpressing Mpped2 cDNA were generated by transfecting a luciferase-expressing vector (the firefly luciferase gene cloned in the plentiV5 vector; Invitrogen) into the stable Mpped2 clone or into the control empty vector clone (bioluminescence photon/s emission data and standard curves reported in **Fig. S2A and B**). Then 1 x 10^6 Ctr-pluc2 or Mpped2-9-pLuc cells were mixed with 15 μL PBS and injected into the left adrenal glands of the mice, as previously reported in reference 63. Briefly, 16 nude/SCID mice (Harlan Laboratories) were anesthetized using avertin (Sigma Aldrich) as a 3% solution in tert-amyl alcohol (Fisher) at a dose of 3 mg per 10 g body weight. These mice were then injected with the cells after laparatomy into the capsule of the left adrenal gland. The mice were monitored at least once a week for evidence of tumor development by bioluminescence acquisition (IVIS200-Calipers life science, Xenogen) and for evidence of tumor-associated morbidity. For these BLI acquisitions, the mice were anesthetized with isofluorane and injected with 100 μL D-luciferin (of a 15 mg/mL stock) per 10 g body weight. Ten minutes after this luciferin injection, the mice were imaged for 30 sec, with two acquisitions per mouse (ventral, dorsal). To quantify the bioluminescence, regions were drawn that encircled the luciferase-emitting areas of each mouse. The integrated fluxes of photons (photons/s) within each area of interest (BLI signals) were determined using the Living Images Software Package 3.0 (Caliper). The emission data from when the tumors started growing were collected for at least 6 weeks, and they were normalized to the BLI signals on the day of the cell injections.

All of the animal work was conducted according to the relevant national and international guidelines. Approval was obtained from the Institutional Animal Care and Ethical Committee at CEINGE and the 'Federico II' University of Naples, according to Protocol #29 of 30/09/2009, and the Italian Ministry of Health, Dipartimento Sanità Pubblica Veterinaria D.L. 116/92, confirming that all of the experiments performed conformed to the relevant regulatory standards.

Disclosure of Potential Conflicts of Interest

All of the authors declare that they no financial or personal relationships with other people or organizations that could inappropriately influence their work.

Acknowledgements

The authors would like to thank: Prof. Luigi Del Vecchio and the cell cycle facility at CEINGE, Naples, for analysis of the cell cycle data and the Oligonucleotides Synthesis Facility at CEINGE, Naples for the *sh*-interference ribonucleotide synthesis.

Role of the Funding Sources

This study was supported by the Associazione Open Oncologia Pediatrica e Neuroblastoma (Fellowship to V.A), FP6-E.E.T pipeline LSH-CT-2006-037260 (M.Z.), FP7-Tumic HEALTH-F2-2008-201662 (M.Z.), Grant AIRC 2007 (M.Z.), Associazione Italiana contro la lotta al Neuroblastoma "Progetto Pensiero" (A.I. and M.Z.).

Note

Supplemental materials can be found at:
www.landesbioscience.com/journals/cc/article/19063

References

1. Maris JM, Hogarty MD, Bagatell R, Cohn SL. Neuroblastoma. Lancet 2007; 369:2106-20; PMID:17586306; http://dx.doi.org/10.1016/S0140-6736(07)60983-0.
2. Maris JM, Matthay KK. Molecular biology of neuroblastoma. J Clin Oncol 1999; 17:2264-79; PMID:10561284.
3. Bown N. Neuroblastoma tumour genetics: clinical and biological aspects. J Clin Pathol 2001; 54:897-910; PMID:11729208; http://dx.doi.org/10.1136/jcp.54.12.897.
4. D'Angio GJ, Evans AE, Koop CE. Special pattern of widespread neuroblastoma with a favourable prognosis. Lancet 1971; 297:1046-9; PMID:4102970; http://dx.doi.org/10.1016/S0140-6736(71)91606-0.
5. Vermeulen J, De Preter K, Mestdagh P, Laureys G, Speleman F, Vandesompele J. Predicting outcomes for children with neuroblastoma. Discov Med 2010; 10:29-36; PMID:20670596.
6. Sidell N. Retinoic acid-induced growth inhibition and morphologic differentiation of human neuroblastoma cells in vitro. J Natl Cancer Inst 1982; 68:589-96; PMID:7040765.
7. Reynolds CP, Matthay KK, Villablanca JG, Maurer BJ. Retinoid therapy of high-risk neuroblastoma. Cancer Lett 2003; 197:185-92; PMID:12880980; http://dx.doi.org/10.1016/S0304-3835(03)00108-3.
8. Matthay KK, Seeger RC, Reynolds CP, Stram DO, O'Leary M, Harris RE, et al. Comparison of autologous and allogeneic bone marrow transplantation for neuroblastoma. Prog Clin Biol Res 1994; 385:301-7; PMID:7972225.
9. Rana B, Veal GJ, Pearson AD, Redfern CP. Retinoid X receptors and retinoid response in neuroblastoma cells. J Cell Biochem 2002; 86:67-78; PMID:12112017; http://dx.doi.org/10.1002/jcb.10192.
10. Matthay KK, Villablanca JG, Seeger RC, Stram DO, Harris RE, Ramsay NK, et al. Children's Cancer Group. Treatment of high-risk neuroblastoma with intensive chemotherapy, radiotherapy, autologous bone marrow transplantation and 13-cis-retinoic acid. N Engl J Med 1999; 341:1165-73; PMID:10519894; http://dx.doi.org/10.1056/NEJM199910143411601.
11. Seeger RC, Siegel SE, Sidell N. Neuroblastoma: clinical perspectives, monoclonal antibodies and retinoic acid. Ann Intern Med 1982; 97:873-84; PMID:6756240.
12. Reynolds CP, Kane DJ, Einhorn PA, Matthay KK, Crouse VL, Wilbur JR, et al. Response of neuroblastoma to retinoic acid in vitro and in vivo. Prog Clin Biol Res 1991; 366:203-11; PMID:2068138.
13. Sucov HM, Evans RM. Retinoic acid and retinoic acid receptors in development. Mol Neurobiol 1995; 10:169-84; PMID:7576306; http://dx.doi.org/10.1007/BF02740674.
14. Ohira M, Oba S, Nakamura Y, Isogai E, Kaneko S, Nakagawa A, et al. Expression profiling using a tumor-specific cDNA microarray predicts the prognosis of intermediate risk neuroblastomas. Cancer Cell 2005; 7:337-50; PMID:15837623; http://dx.doi.org/10.1016/j.ccr.2005.03.019.
15. Hiyama E, Hiyama K, Yamaoka H, Sueda T, Reynolds CP, Yokoyama T. Expression profiling of favorable and unfavorable neuroblastomas. Pediatr Surg Int 2004; 20:33-8; PMID:14691637; http://dx.doi.org/10.1007/s00383-003-1077-3.
16. Ohira M, Morohashi A, Inuzuka H, Shishikura T, Kawamoto T, Kageyama H, et al. Expression profiling and characterization of 4,200 genes cloned from primary neuroblastomas: identification of 305 genes differentially expressed between favorable and unfavorable subsets. Oncogene 2003; 22:5525-36; PMID:12934113; http://dx.doi.org/10.1038/sj.onc.1206853.
17. Riley RD, Heney D, Jones DR, Sutton AJ, Lambert PC, Abrams KR, et al. A systematic review of molecular and biological tumor markers in neuroblastoma. Clin Cancer Res 2004; 10:4-12; PMID:14734444; http://dx.doi.org/10.1158/1078-0432.CCR-1051-2.
18. Wei JS, Greer BT, Westermann F, Steinberg SM, Son CG, Chen QR, et al. Prediction of clinical outcome using gene expression profiling and artificial neural networks for patients with neuroblastoma. Cancer Res 2004; 64:6883-91; PMID:15466177; http://dx.doi.org/10.1158/0008-5472.CAN-04-0695.
19. Takita J, Ishii M, Tsutsumi S, Tanaka Y, Kato K, Toyoda Y, et al. Gene expression profiling and identification of novel prognostic marker genes in neuroblastoma. Genes Chromosomes Cancer 2004; 40:120-32; PMID:15101045; http://dx.doi.org/10.1002/gcc.20021.
20. Bonetta L, Kuehn SE, Huang A, Law DJ, Kalikin LM, Koi M, et al. Wilms tumor locus on 11p13 defined by multiple CpG island-associated transcripts. Science 1990; 250:994-7; PMID:2173146; http://dx.doi.org/10.1126/science.2173146.
21. Gessler M, Poustka A, Cavenee W, Neve RL, Orkin SH, Bruns GA. Homozygous deletion in Wilms tumours of a zinc-finger gene identified by chromosome jumping. Nature 1990; 343:774-8; PMID:2154702; http://dx.doi.org/10.1038/343774a0.
22. Schwartz F, Neve R, Eisenman R, Gessler M, Bruns G. A WAGR region gene between PAX-6 and FSHB expressed in fetal brain. Hum Genet 1994; 94:658-64; PMID:7527372; http://dx.doi.org/10.1007/BF00206960.
23. Schwartz F, Ota T. The 239AB gene on chromosome 22: a novel member of an ancient gene family. Gene 1997; 194:57-62; PMID:9266672; http://dx.doi.org/10.1016/S0378-1119(97)00149-2.
24. Richter W. 3',5' Cyclic nucleotide phosphodiesterases class III: members, structure and catalytic mechanism. Proteins 2002; 46:278-86; PMID:11835503; http://dx.doi.org/10.1002/prot.10049.
25. Conti M, Beavo J. Biochemistry and physiology of cyclic nucleotide phosphodiesterases: essential components in cyclic nucleotide signaling. Annu Rev Biochem 2007; 76:481-511; PMID:17376027; http://dx.doi.org/10.1146/annurev.biochem.76.060305.150444.
26. Mehats C, Andersen CB, Filopanti M, Jin SL, Conti M. Cyclic nucleotide phosphodiesterases and their role in endocrine cell signaling. Trends Endocrinol Metab 2002; 13:29-35; PMID:11750860; http://dx.doi.org/10.1016/S1043-2760(01)00523-9.
27. Imamura R, Yamanaka K, Ogura T, Hiraga S, Fujita N, Ishihama A, et al. Identification of the cpdA gene encoding cyclic 3',5'-adenosine monophosphate phosphodiesterase in *Escherichia coli*. J Biol Chem 1996; 271:25423-9; PMID:8810311; http://dx.doi.org/10.1074/jbc.271.41.25423.
28. Macfadyen LP, Ma C, Redfield RJ. A 3',5'-cyclic AMP (cAMP) phosphodiesterase modulates cAMP levels and optimizes competence in *Haemophilus influenzae* Rd. J Bacteriol 1998; 180:4401-5; PMID:9721275.
29. Shenoy AR, Sreenath N, Podobnik M, Kovacevic M, Visweswariah SS. The Rv0805 gene from *Mycobacterium tuberculosis* encodes a 3',5'-cyclic nucleotide phosphodiesterase: biochemical and mutational analysis. Biochemistry 2005; 44:15695-704; PMID:16313172; http://dx.doi.org/10.1021/bi0512391.
30. Tyagi R, Shenoy AR, Visweswariah SS. Characterization of an evolutionarily conserved metallophosphoesterase that is expressed in the fetal brain and associated with the WAGR syndrome. J Biol Chem 2009; 284:5217-28; PMID:19004815; http://dx.doi.org/10.1074/jbc.M805996200.
31. Page CP, Spina D. Phosphodiesterase inhibitors in the treatment of inflammatory diseases. Handb Exp Pharmacol 2011; 204:391-414; PMID:21695650; http://dx.doi.org/10.1007/978-3-642-17969-3_17.
32. Bjørgo E, Moltu K, Taskén K. Phosphodiesterases as targets for modulating T-cell responses. Handb Exp Pharmacol 2011; 204:345-63; PMID:21695648; http://dx.doi.org/10.1007/978-3-642-17969-3_15.
33. Hertz AL, Beavo JA. Cyclic nucleotides and phosphodiesterases in monocytic differentiation. Handb Exp Pharmacol 2011; 204:365-90; PMID:21695649; http://dx.doi.org/10.1007/978-3-642-17969-3_16.
34. Das A, Durrant D, Mitchell C, Mayton E, Hoke NN, Salloum FN, et al. Sildenafil increases chemotherapeutic efficacy of doxorubicin in prostate cancer and ameliorates cardiac dysfunction. Proc Natl Acad Sci USA 2010; 107:18202-7; PMID:20884855; http://dx.doi.org/10.1073/pnas.1006965107.
35. Horvath A, Korde L, Greene MH, Libe R, Osorio P, Faucz FR, et al. Functional phosphodiesterase 11A mutations may modify the risk of familial and bilateral testicular germ cell tumors. Cancer Res 2009; 69:5301-6; PMID:19549888; http://dx.doi.org/10.1158/0008-5472.CAN-09-0884.
36. Levy I, Horvath A, Azevedo M, de Alexandre RB, Stratakis CA. Phosphodiesterase function and endocrine cells: links to human disease and roles in tumor development and treatment. Curr Opin Pharmacol 2011; 11:689-97; PMID:22047791; http://dx.doi.org/10.1016/j.coph.2011.10.003.
37. Marino N, Zollo M. Understanding h-prune biology in the fight against cancer. Clin Exp Metastasis 2007; 24:637-45; PMID:17952613; http://dx.doi.org/10.1007/s10585-007-9109-3.
38. De Preter K, Vandesompele J, Menten B, Carr P, Fiegler H, Edsjö A, et al. Positional and functional mapping of a neuroblastoma differentiation gene on chromosome 11. BMC Genomics 2005; 6:97; PMID:16000168; http://dx.doi.org/10.1186/1471-2164-6-97.
39. Miller DJ, Shuvalova L, Evdokimova E, Savchenko A, Yakunin AF, Anderson WF. Structural and biochemical characterization of a novel Mn^{2+}-dependent phosphodiesterase encoded by the yfcE gene. Protein Sci 2007; 16:1338-48; PMID:17586769; http://dx.doi.org/10.1110/ps.072764907.
40. Vogel A, Schilling O, Niecke M, Bettmer J, Meyer-Klaucke W. ElaC encodes a novel binuclear zinc phosphodiesterase. J Biol Chem 2002; 277:29078-85; PMID:12029081; http://dx.doi.org/10.1074/jbc.M112047200.
41. Dermol U, Janardan V, Tyagi R, Visweswariah SS, Podobnik M. Unique utilization of a phosphoprotein phosphatase fold by a mammalian phosphodiesterase associated with WAGR syndrome. J Mol Biol 2011; 412:481-94; PMID:21824479; http://dx.doi.org/10.1016/j.jmb.2011.07.060.
42. Friedman HS, Burger PC, Bigner SH, Trojanowski JQ, Wikstrand CJ, Halperin EC, et al. Establishment and characterization of the human medulloblastoma cell line and transplantable xenograft D283 Med. J Neuropathol Exp Neurol 1985; 44:592-605; PMID:4056828; http://dx.doi.org/10.1097/00005072-198511000-00005.
43. Keles GE, Berger MS, Srinivasan J, Kolstoe DD, Bobola MS, Silber JR. Establishment and characterization of four human medulloblastoma-derived cell lines. Oncol Res 1995; 7:493-503; PMID:8866661.
44. Barnes EN, Biedler JL, Spengler BA, Lyser KM. The fine structure of continuous human neuroblastoma lines SK-N-SH, SK-N-BE(2) and SK-N-MC. In Vitro 1981; 17:619-31; PMID:7327593; http://dx.doi.org/10.1007/BF02618461.
45. Kanda N, Schreck R, Alt F, Bruns G, Baltimore D, Latt S. Isolation of amplified DNA sequences from IMR-32 human neuroblastoma cells: facilitation by fluorescence-activated flow sorting of metaphase chromosomes. Proc Natl Acad Sci USA 1983; 80:4069-73; PMID:6575396; http://dx.doi.org/10.1073/pnas.80.13.4069.
46. Ross RA, Spengler BA, Biedler JL. Coordinate morphological and biochemical interconversion of human neuroblastoma cells. J Natl Cancer Inst 1983; 71:741-7; PMID:6137586.
47. Schwartz F, Eisenman R, Knoll J, Gessler M, Bruns G. cDNA sequence, genomic organization and evolutionary conservation of a novel gene from the WAGR region. Genomics 1995; 29:526-32; PMID:8666403; http://dx.doi.org/10.1006/geno.1995.9973.

48. D'Angelo A, Garzia L, André A, Carotenuto P, Aglio V, Guardiola O, et al. Prune cAMP phosphodiesterase binds nm23-H1 and promotes cancer metastasis. Cancer Cell 2004; 5:137-49; PMID:14998490; http://dx.doi.org/10.1016/S1535-6108(04)00021-2.
49. Campostrini N, Pascali J, Hamdan M, Astner H, Marimpietri D, Pastorino F, et al. Proteomic analysis of an orthotopic neuroblastoma xenograft animal model. J Chromatogr B Analyt Technol Biomed Life Sci 2004; 808:279-86; PMID:15261822; http://dx.doi.org/10.1016/j.jchromb.2004.05.013.
50. Shai R, Shi T, Kremen TJ, Horvath S, Liau LM, Cloughesy TF, et al. Gene expression profiling identifies molecular subtypes of gliomas. Oncogene 2003; 22:4918-23; PMID:12894235; http://dx.doi.org/10.1038/sj.onc.1206753.
51. Wang Q, Diskin S, Rappaport E, Attiyeh E, Mosse Y, Shue D, et al. Integrative genomics identifies distinct molecular classes of neuroblastoma and shows that multiple genes are targeted by regional alterations in DNA copy number. Cancer Res 2006; 66:6050-62; PMID:16778177; http://dx.doi.org/10.1158/0008-5472.CAN-05-4618.
52. Asgharzadeh S, Pique-Regi R, Sposto R, Wang H, Yang Y, Shimada H, et al. Prognostic significance of gene expression profiles of metastatic neuroblastomas lacking MYCN gene amplification. J Natl Cancer Inst 2006; 98:1193-203; PMID:16954472; http://dx.doi.org/10.1093/jnci/djj330.
53. Chang GC, Hsu SL, Tsai JR, Liang FP, Lin SY, Sheu GT, et al. Molecular mechanisms of ZD1839-induced G_1-cell cycle arrest and apoptosis in human lung adenocarcinoma A549 cells. Biochem Pharmacol 2004; 68:1453-64; PMID:15345335; http://dx.doi.org/10.1016/j.bcp.2004.06.006.
54. Bardon S, Foussard V, Fournel S, Loubat A. Monoterpenes inhibit proliferation of human colon cancer cells by modulating cell cycle-related protein expression. Cancer Lett 2002; 181:187-94; PMID:12175534; http://dx.doi.org/10.1016/S0304-3835(02)00047-2.
55. Oliver TG, Grasfeder LL, Carroll AL, Kaiser C, Gillingham CL, Lin SM, et al. Transcriptional profiling of the Sonic hedgehog response: a critical role for N-myc in proliferation of neuronal precursors. Proc Natl Acad Sci USA 2003; 100:7331-6; PMID:12777630; http://dx.doi.org/10.1073/pnas.0832317100.
56. Baek SH, Kioussi C, Briata P, Wang D, Nguyen HD, Ohgi KA, et al. Regulated subset of G_1 growth-control genes in response to derepression by the Wnt pathway. Proc Natl Acad Sci USA 2003; 100:3245-50; PMID:12629224; http://dx.doi.org/10.1073/pnas.0330217100.
57. Kioussi C, Briata P, Baek SH, Rose DW, Hamblet NS, Herman T, et al. Identification of a Wnt/Dvl/beta-Catenin→Pitx2 pathway mediating cell-type-specific proliferation during development. Cell 2002; 111:673-85; PMID:12464179; http://dx.doi.org/10.1016/S0092-8674(02)01084-X.
58. Suzui M, Masuda M, Lim JT, Albanese C, Pestell RG, Weinstein IB. Growth inhibition of human hepatoma cells by acyclic retinoid is associated with induction of p21(CIP1) and inhibition of expression of cyclin D1. Cancer Res 2002; 62:3997-4006; PMID:12124333.
59. Finn SP, Smyth P, Cahill S, Streck C, O'Regan EM, Flavin R, et al. Expression microarray analysis of papillary thyroid carcinoma and benign thyroid tissue: emphasis on the follicular variant and potential markers of malignancy. Virchows Arch 2007; 450:249-60; PMID:17252232; http://dx.doi.org/10.1007/s00428-006-0348-5.
60. Mazzanti C, Zeiger MA, Costouros NG, Umbricht C, Westra WH, Smith D, et al. Using gene expression profiling to differentiate benign versus malignant thyroid tumors. Cancer Res 2004; 64:2898-903; PMID:15087409; http://dx.doi.org/10.1158/0008-5472.CAN-03-3811.
61. Seitz S, Korsching E, Weimer J, Jacobsen A, Arnold N, Meindl A, et al. Genetic background of different cancer cell lines influences the gene set involved in chromosome 8 mediated breast tumor suppression. Genes Chromosomes Cancer 2006; 45:612-27; PMID:16552773; http://dx.doi.org/10.1002/gcc.20325.